Denoising preterm EEG by signal decomposition and adaptive filtering: A comparative study

X Navarro, F Porée, A Beuchée, G Carrault

Denoising preterm EEG by signal decomposition and adaptive filtering: A comparative study

X. Navarro[1,2,3], F. Porée[1,2], A. Beuchée[1,2,4], G. Carrault[1,2,5]

[1]INSERM, U1099, Rennes, F-35000, France;

[2]Université de Rennes 1, Laboratoire Traitement du Signal et de l'Image, Rennes, F-35000, France;

[3]Sorbonne Universités, UPMC Univ Paris 06, INSERM, UMRS 1158, Neurophysiologie Respiratoire Expérimentale et Clinique, Paris, F-75005, France

[4]CHU Rennes, Pôle Médico-Chirurgical de Pédiatrie et de Génétique Clinique, Rennes, F-35000, France

[5]INSERM, CIC 1414, Rennes, F-35000, France

Abstract

Electroencephalography (EEG) from preterm infants' monitoring systems is usually contaminated by several sources of noise that have to be removed in order to correctly interpret signals and perform automated analysis reliably. Band-pass and adaptive filters (AF) continue to be systematically applied, but their efficacy may be decreased facing preterm EEG patterns such as the tracé alternant and slow delta-waves. In this paper, we propose the combination of EEG decomposition with AF to improve the overall denoising process. Using artificially contaminated signals from real EEGs, we compared the quality of filtered signals applying different decomposition techniques: the discrete wavelet transform, the empirical mode decomposition (EMD) and a recent improved version, the complete ensemble EMD with adaptive noise. Simulations demonstrate that introducing EMD-based techniques prior to AF can reduce up to 30% the root mean squared errors in denoised EEGs.

Keywords: Electroencephalography; Empirical mode decomposition; Mode mixing; Adaptive filter; Preterm infants

1 Introduction

Brain monitoring, based on a simplified electroencephalographic (EEG) montage, adds complementary and crucial information to the cardio-respiratory monitoring in the Neonatal Intensive Care Unit (NICU). Composed by one (two electrodes) or two channels (four electrodes), this EEG set-up provides simplicity, reasonable cost and direct information about the neurological status of the infant and is usually time-compressed and visualized as amplitude-integrated EEG [1]. As multiple sources of noise contaminate the EEG and a clean signal is mandatory for clinical interpretation [2], the design of a strategy to remove correctly the artifacts becomes challenging.

*Address for correspondence: Neurophysiologie Respiratoire Expérimentale et Clinique, Hôpital de la Pitié Salpêtrière, 91 Boulevard de l'Hôpital, 75013 Paris.

✉: xavier.navarro@upmc.com

Particularly, the elimination of cardiac artifacts requires adapted solutions since their power spectral density overlaps θ, α and β EEG bands (4-30 Hz). When interferences and the electrocardiogram (ECG) have similar waveforms, a robust and simple solution can be found by adaptive filters (AF) using the recorded ECG as a reference [3]. However, as the effectiveness of AF may decrease under non-stationary conditions, sub-band or wavelet-based filtering emerged as well as alternatives to improve filters performance [4, 5].

More sophisticated EEG denoising techniques based on signal decomposition were proposed later on. For instance, independent component analysis (ICA), performs decompositions in a prescribed number of components, one of them containing, presumably, the unwanted ECG artifact [6, 7]. However, the efficiency of the denoising process depends on the availability of several derivations and on the accomplishment of certain assumptions on the signals. Constrained by our one/two-channel EEG, these approaches have not been exploited in the present work.

A relatively new decomposition technique, the empirical mode decomposition (EMD) [8], has been found to be very advantageous to decompose nonstationary signals in intrinsic mode functions (IMFs). The quality of the separation in noisy signals has even been improved with the latest versions, first the ensemble EMD (EEMD) [9] and then the complete EEMD with adaptive noise (CEEMDAN) [10]. Their application to remove artifacts has been widely applied, as for instance, performing EMD on noisy ECG signals and then removing the IMFs dominated by noise [11], or even combining EMD with ICA [12, 13]. In a preliminary study, we proposed the combination of EMD and adaptive filtering to remove cardiac noise in preterm electroencephalogram [14]. In the present paper, we provide more insights about this approach, analyzing in detail the parameters leading to the best performances and how these are affected by mode mixing, a well-known limitation of EMD [9]. Additionally, we compare the performance of EMD-based techniques to clean neonatal EEG with the use of discrete wavelet transform (DWT) as a decomposition alternative.

2 Description of the denoising framework

The proposed framework consists on the six-step straightforward method described in Figure 1. Given an input signal, $x(n), n = 1 \dots N$, corresponding to the noisy EEG:

1. Obtain M independent subcomponents $x_k(n), k = 1 \dots M$ by performing decomposition. They correspond to sub-bands or to IMFs if DWT or EMD/CEEMDAN are chosen, respectively.

2. Estimate the main average frequency of each subcomponent (f_k) from its power spectral density (PSD).

3. Find f_e from the ECG reference, $z(n)$. This frequency splits the ECG PSD in 5% on the left and 95% on the right, so that the range [0 - f_e] Hz is considered to have a non significant portion of the ECG energy.

4. Obtain $x_H(n)$, a signal formed by the addition of subcomponents having $f_k \geq f_e$ and $x_L(n)$, the component adding those subcomponents carrying δ-waves, i.e $0.5 \leq f_k < f_e$. The limit imposed by 0.5 Hz responds to both clinical and technical criteria, that is, a trade-off between the inclusion of very slow EEG patterns and the minimization of low-frequency noise (LFN). Consequently, the remaining subcomponents ($f_k < 0.5$ Hz) are rejected.

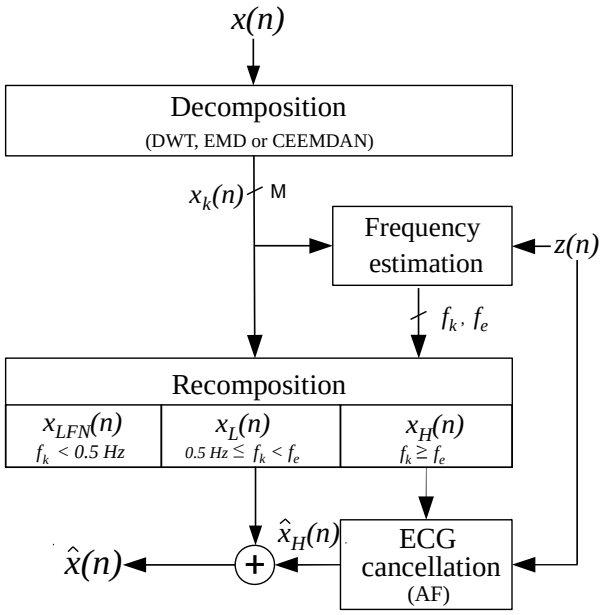

Figure 1: Block diagram of the proposed methodology with different options to decompose the EEG.

5. Remove ECG noise in $x_H(n)$ using the recorded ECG as a reference and obtain the cleaned component, $\widehat{x}_H(n)$. To this end, adaptive filtering can be performed because the cardiac artifacts appearing in newborns' EEG are similar to the ECG originated in the chest [15].

6. Reconstruct the clean EEG, $\widehat{x}(n)$, by the addition of $x_L(n)$ and $\widehat{x}_H(n)$.

3 Methods

3.1 EEG decomposition by the discrete wavelet transform

The wavelet transform is a very useful and popular analysis tool for time-scale representation and decomposition of non-stationary signals (for a complete survey about the theory of wavelets, the interested reader can refer to [16]). By means of the DWT, the decomposition can be performed so that the frequencies are in a power of two scale, a procedure also known as multi resolution analysis (MRA).

3.2 EEG decomposition by empirical mode decomposition

The application of empirical mode decomposition yields the so-called intrinsic modal functions [8], a number of subcomponents that must satisfy two conditions: 1) the number of extrema and zero-crossing must be equal or differ at most by one, and 2) the mean value of the upper and lower envelopes must be zero. Then, the unmixing process, also called sifting, can be performed:

1. Find local minima and maxima of the input signal, $x(n)$.

2. Form upper, $e_u(n)$, and lower, $e_l(n)$, envelopes by cubic splines interpolation.

3. Find the mean, $m(n) = \frac{e_u(n)+e_l(n)}{2}$.

4. Compute $h_1(n) = x(n) - m(n)$. If h_1 is not an IMF, the procedure is repeated from step 1 using this signal instead of $x(n)$. Else, $h_1(n) = IMF_1(n)$.

5. If the residue, $res_1(n) = x(n) - IMF_1(n)$ has more than a zero cross, go to step 1 and find next IMF.

The procedure continues until the last residue, $res_M(n)$ has no zero crossings or some stopping criteria is fulfilled. This residual component has the lowest frequency content of the time-series. Once $IMF_k(n)$ are extracted, the signal can be expressed as:

$$x(n) = \sum_{k=1}^{M} IMF_k(n) + res_M(n). \tag{1}$$

3.3 Complete ensemble EMD with adaptive noise

The decomposition of noisy signals using EMD may result in mode mixing or corruption of modes, i.e. the presence of one oscillation in different IMFs. The ensemble EMD [9] was introduced to overcome this problem by repeating decompositions R times and adding white noise to the signal:

$$x^r(n) = x(n) + w_r(n), \quad r = 1, .., R \tag{2}$$

where $w_r(n)$ are different realizations of white noise with variance ε, producing $IMF_k^r(n)$. Then, the final oscillatory modes are obtained by averaging:

$$\overline{IMF}_k(n) = \frac{1}{R}\sum_{r=1}^{R} IMF_k^r(n) \tag{3}$$

This procedure improves the quality of the separation, but at the expenses of a high computational cost, and without the warranty of a perfect reconstruction of the signal because a different number of IMFs may be obtained for each iteration.

The complete EEMD with adaptive noise (CEEMDAN) was proposed to ameliorate the spectral separation of modes and to reduce computational time [10]. In EEMD each $x^r(n)$ is decomposed independently and R residuals are obtained. The CEEMDAN computes the first decomposition by averaging the R IMFs and a unique first residue is retained:

$$res_1(n) = x(n) - \overline{IMF_1'}(n), \tag{4}$$

where $\overline{IMF_1'}(n)$ is the same as the first IMF obtained by EEMD Then, EMD is performed over a set of signals obtained by adding different noise realizations to $res_1(n)$, so the next IMF – noted here $\overline{IMF_2'}(n)$ – is found by averaging the corresponding set of IMFs. The corresponding residue is $res_2(n) = res_1(n) - \overline{IMF_2'}(n)$, and so on, until the stopping criterion is achieved. Once $\overline{IMF_k'}(n)$ and a final residue are obtained, $x(n)$ can be reassembled by their addition similarly than in Equation 1.

3.4 Adaptive filtering

Adaptive filtering has been extensively applied to cancel cardiac artifacts in biomedical signals using the recorded ECG as a reference [21]. In our denoising framework, we implemented the recursive least square algorithm (RLS) as it provides faster convergences than the classic least mean squares [22].

4 Validation strategy

To validate the efficacy of the different denoising options, contaminated signals were generated from real recordings. Data came from 30 preterm infants (36 to 39 weeks post-menstrual age) born at the University Hospital of Rennes (France). ECG and double-channel EEG (Fp1-T3, Fp2-T4) were acquired originally at 512 Hz sampling frequency, low-pass filtered (40 Hz cut-off) and subsampled to 128 Hz.

Since EEG signals acquired NICUs can also be contaminated with low frequency noise, we constructed two groups to simulate realistic conditions:

1. Group 1: Thirty EEG excerpts with added ECG noise (filtering recorded EEG by a 21th-order FIR filter with random coefficients) with signal-to-noise ratios (SNRs) ranging from -5 to 10 dB in steps of 5.

2. Group 2: Thirty EEG excerpts with added ECG at 5dB SNR plus LFN at variable SNR. To emulate breathing and other slow movements, that may appear spontaneously and discontinuously, LFN noise consisted in one cycle of a sinusoidal wave, very close to the limit of the delta band, fixed randomly between 0.3 and 0.5 Hz. The power of the wave was set to obtain SNRs (relative to the original signal) ranging from -10 to 10 dB in steps of 5 dB.

Excerpts were selected by an experienced clinician, ensuring the absence of artifacts and including different EEG neonatal patterns. The amplitude of the noisy components was properly modified to obtain SNRs according to the following equation:

$$SNR = 10 \log \frac{P_{EEG}}{P_{noise}} \tag{5}$$

where P_{EEG} and P_{noise} are the power of an original EEG excerpt and the power of the added artifacts, respectively. Some examples of artificially contaminated EEG signals are shown in Figure 2.

After processing separately each noisy EEG excerpt, $x(n)$, by the denoising framework, the quality of the different decomposition options described in Figure 1 is measured in terms of root mean squared error (RMSE):

$$\text{RMSE} = \sqrt{\frac{1}{N} \sum_{n=1}^{N} [x_o(n) - \widehat{x}(n)]^2} \tag{6}$$

where $x_o(n)$ is the original, uncorrupted EEG, $\widehat{x}(n)$ is the cleaned signal and N is the number of samples in each excerpt.

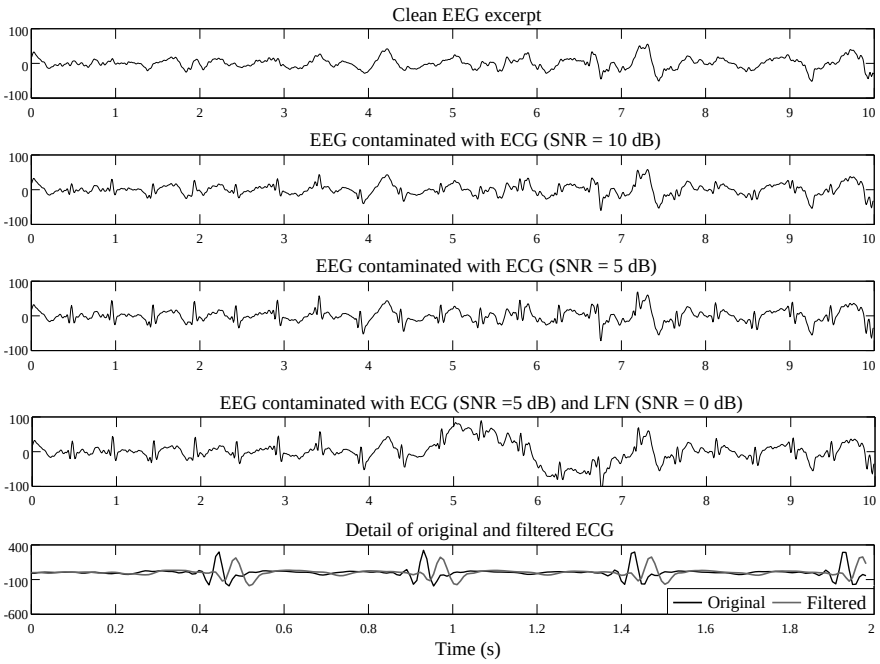

Figure 2: Example of the generation of artificially contaminated EEGs by the filtered ECG and LFN. Using the first signal (clean EEG), two examples of Group 1 (second and third signals) have been formed. The fourth signal (a Group 2 example) is formed by the addition of the third signal and LFN at 0 dB. The lower plot shows the originally recorded ECG, $z(n)$, and the ECG noise obtained by applying the 21st-order FIR filter.

5 Tuning of parameters

5.1 Filtering and decomposition

To find the appropriate parameters for the different techniques, some preliminary tests were carried out. Firstly, we found the appropriate order and algorithm of the adaptive filter in our particular signals. A filter order L=16 and a forgetting factor $\lambda = 1 - \frac{1}{10L}$ (as suggested by Eleftheriou and Falconer [22]) yielded the best results.

The DWT was performed using 6th order Daubechies wavelet [17], a choice with satisfactory results in these signals [18]. The MRA framework was configured to obtain seven levels of successive details and the approximation interval, yielding eight subcomponents with their frequency intervals between 32-64, 16-32, 8-16, 4-8, 2-4, 1-2, 0.5-1 and <0.5 Hz, that corresponded to LFN.

The EMD was computed by an efficient algorithm [19] that introduces two thresholds (θ_1 and θ_2) in the second criterion to consider an IMF, and a tolerance factor, $\alpha \in [0, 1]$. They aim at guaranteeing globally small fluctuations in the mean while taking into account locally large excursions. Finally, the CEEMDAN was performed by a recent algorithm improvement that optimizes speed and enhances quality with respect to its previous version [20].

5.2 Study of mode mixing

As mentioned before, subcomponents obtained by EMD-based techniques can suffer mode mixing, however, this phenomenon is not a major concern as far as it mixes frequencies from only one side

of the separation determined by f_e. In this case, the sum of the IMFs yielding $x_L(n)$ and $x_H(n)$ should be the same as in the absence of mode mixing. More attention needs to be paid to those IMFs having frequency tones on both sides of the f_e boundary, in particular:

1. Modes with $f_k \geq f_e$ –summed in $x_H(n)$– containing oscillations below f_e. Since $x_H(n)$ is processed by the AF, these low frequencies may lead to underperform the ECG cancellation.

2. Modes with $0.5 \leq f_k < f_e$ containing frequencies above f_e. The ECG noise could be partially installed in $x_L(n)$ so it would be unprocessed by the AF and incompletely removed in the final reassembled signal.

These two cases will be subsequently referred as to critical mixing I and II, respectively. Figure 3 shows frequencies contained in IMFs performing EMD in a real EEG. The two first IMFs clearly exhibit mode mixing, but since it occurs beyond the limit of f_e, it has no consequences on the denoising process. The energies carried by frequencies in the lower whiskers of IMF_1, IMF_2 and IMF_3 crossing the horizontal dashed line constitute critical mixing I. Likewise, the energies in the frequencies crossing f_e in IMF_4 determine critical mixing II.

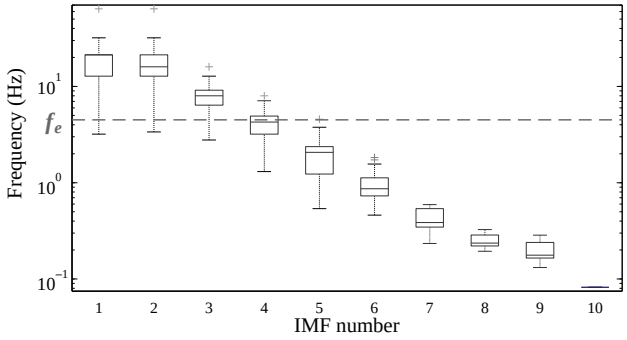

Figure 3: Frequencies contained in all IMFs performing EMD in a real EEG. IMF_1 and IMF_2 contain almost identical frequencies, evidencing mode mixing. The small frequency portions below f_e of IMF_1, IMF_2 and IMF_3 can be considered as critical mixing I, and conversely, the portion of IMF_4 exceeding f_e can be accounted as critical mixing II.

To quantify critical mixing we took advantage of the IMFs to characterize the frequency and amplitude of the components. To illustrate this idea, let us consider an IMF with a single zero-crossing. Since the oscillation of this signal completes an entire period, its frequency can be obtained by simply computing the inverse of the cycle time. Even if decompositions of experimental signals do not yield pure tones, this operation can approximate the frequencies describing cycles within an IMF.

Therefore, if a k-th IMF is composed by C_k cycles, with frequencies f_k^l ($l = 1 \dots C_k$), the total energy of the cycles into the critical mixing I region, CM_I, can be expressed as:

$$CM_I = \sum_{\substack{k \\ f_k \geq f_e}} \sum_{\substack{l=1 \\ f_k^l \geq f_e}}^{C_k} \left\| IMF_k^l(n) \right\|^2 \tag{7}$$

Table 1: Decomposition parameters for EMD (θ_1, α) and CEEMDAN (ε) minimizing critical mixing in ten examples from Group 1 (G1) and Group 2 (G2). The average number of IMFs (M) is also shown.

SNRs for EMD	θ_1	α	M	CM_I (%)	CM_{II} (%)
G1 (-5 dB)	0.03	0.03	9.80 ± 0.42	1.62 ± 0.56	0.63 ± 0.24
G1 (5 dB)	0.02	0.01	10.3 ± 0.48	1.44 ± 1.18	1.57 ± 1.12
G2 (-5 dB)	0.03	0.02	10.1 ± 0.31	0.63 ± 0.52	0.64 ± 0.51
G2 (5 dB)	0.03	0.02	10.3 ± 0.58	0.97 ± 0.62	0.32 ± 0.03
SNRs for CEEMDAN		ε			
G1 (-5 dB)		0.25	9.62 ± 0.52	0.94 ± 0.60	0.06 ± 0.02
G1 (5 dB)		0.90	10.1 ± 0.55	1.46 ± 1.68	0.03 ± 0.02
G2 (-5 dB)		0.35	10.2 ± 0.05	0.24 ± 0.11	0.01 ± 0.01
G2 (5 dB)		0.95	9.80 ± 0.44	0.67 ± 0.57	0.04 ± 0.02

where the first summation includes those IMFs having their main frequency below f_e and $\left\|IMF_k^l(n)\right\|$ is the norm of the l-th cycle in the k-th IMF. Equivalently, for critical mixing II:

$$CM_{II} = \sum_{\substack{k \\ 0.5 \leq f_k < f_e}} \sum_{\substack{l=1 \\ f_k^l < f_e}}^{C_k} \left\|IMF_k^l(n)\right\|^2 \tag{8}$$

CM_I and CM_{II} were then divided by the sum the energies contained in all IMFs to obtain the relative portion of critical mixing in each signal.

Several simulations were performed to find the decomposition parameters minimizing critical mixing at different noise levels. In a first test, ten randomly selected signals from Group 1 were contaminated with -5 dB and 5 dB SNR of cardiac noise and decomposed by both types of EMD. This test was then repeated using ten signals from Group 2, but contaminated with -5 dB and 5 dB SNR LFN. In order to prevent the sifting process from over-iteration and avoid over-decomposition of the signal, it is suggested by Rilling et al. [19] to use the default values $\theta_1 = 0.05$, $\theta_2 = 10\theta_1$ and $\alpha = 0.05$. We therefore modified θ_1 and α from 0.01 to 0.1 in steps of 0.005 to evaluate their effect on critical mixing.

In CEEMDAN, ε was modified from 0.05 to 1 in steps of 0.05 and R was fixed to 50, a choice providing an optimal computational time with negligible reconstruction error [20].

The values of the parameters leading to minimal ratios of critical mixing have been depicted in Table 1. From these tests, it can be stated that CEEMDAN reduces significantly CM_{II}, thus more effective to remove cardiac artifacts. We stated as well that the decomposition parameters (especially ε [9]) depend on the noise levels of contaminated signals and, hence, they should be adjusted increasingly as the EEG signals become more noisy to reduce critical mixing.

6 Results and discussion

6.1 ECG removal

The results of denoising Group 1 are summarized in Table 2. Indeed, the application of signal decomposition techniques before the adaptive filter resulted in a general decrease of the RMSEs compared to denoising without EEG decomposition. However, this gain of quality was unequally

distributed and statistically significant only for certain SNRs. CEEMDAN provided in average a 30% reduction of RMSEs whereas EMD and DWT resulted in 7.3% and 3.4% respective reductions.

It is noteworthy to mention that high SNR levels are then more favorable to perform EEG signal decomposition, probably due to smaller distortion introduced to the final reconstructed signal when only the noisy part of the EEG is processed by the AF. On the contrary, in low SNRs the denoising performances of all methods converge because useful information is masked by noise and decomposition become less effective.

6.2 ECG and low frequency noise removal

The scenario in which signals also contain low frequency noise has been evaluated using data from Group 2. To compare the improvements of introducing EEG decompositions, we processed the raw signals using a finite impulsional response (FIR) filter with a cutoff frequency of 0.5 Hz before applying the cancellation of ECG noise. This high-pass filter (HPF) can prevent phase distortion, but employing a high order (382) that introduced delay (>1.5 s).

As it can be stated in Table 2, to remove simultaneously LFN and ECG noise only EMD-based decompositions are advantageous in all noise levels, with a 6.7% average RMSE reduction for EMD and 13% for CEEMDAN.

6.3 Denoising real signals

Finally, we performed some tests on real signals, contaminated both with ECG and LFN. To evaluate quantitatively the noise elimination, we employed the artifact rejection ratio (ARR), defined as the ratio of the power of the removed artifacts to the cleaned EEG [23]:

$$ARR = \frac{\sum_{n=1}^{N}[x(n) - \widehat{x}(n)]^2}{\sum_{n=1}^{N}\widehat{x}^2(n)} \tag{9}$$

where $x(n)$ and $\widehat{x}(n)$ are the real EEG before and after the denoising process, respectively.

Since ARR gives information of the whole denoising process (comprising low frequency and cardiac noise), we computed this ratio in small windows surrounding the QRS-peak instants (50 ms) on the noisy excerpt and on the cleaned one. This parameter, ARR_{qrs}, is conceived to give a quantitative idea of how attenuated are the heartbeat artifacts.

The metrics ARR and ARR_{qrs} were computed on the selected excerpts (see Table 2), contaminated with ECG artifacts and low frequency noise. As it can be noticed, the overall noise removal given by ARR and ARR_{qrs} is greater using CEEMDAN. Of note, decomposition techniques are not always advantageous to suppress QRS artifacts, as is the case of DWT and EMD. They provided the lowest ARR_{qrs} values probably for an incomplete separation of $x_H(n)$ before the ECG cancellation takes place.

7 Conclusion

The results presented in this paper show that, in general, EMD-based techniques performed better than DWT decomposition in the EEG signals studied here. This is probably due to the use

Table 2: Results from denoising simulated and real signals. For simulated EEG (both G1 and G2), the efficacy of the different denoising options is expressed as RMSEs (mean ± std. dev.). Best values (lower RMSEs) are in bold. In brackets, the improvement percentages compared to the simple usage of the adaptive filter ("NO DEC" columns) or adaptive filter plus high-pass filter ("NO DEC + HPF"). A Wilcoxon signed rank test compared "NO DEC (+HPF)" with the three decomposition solutions (* denote statistically significant differences at $p < 0.05$). The last two rows show the noise removal estimation by the ARR metrics. Best values (greatest ARR) are highlighted in bold.

G1 simulated signals (SNRs)	NO DEC	DWT	EMD	CEEMDAN
-5 dB	18.8 ± 6.06	18.5 ± 6.06 (1.6%)	18.4 ± 6.00 (2.1%)	**17.2 ± 5.78** (8.6%)
0 dB	10.7 ± 3.41	10.4 ± 3.36 (2.8%)	10.3 ± 3.35 (3.7%)	**8.12 ± 3.13***(25%)
5 dB	6.23 ± 1.95	6.01 ± 1.93 (3.5%)	5.80 ± 1.86 (6.9%)	**3.94 ± 1.74***(36%)
10 dB	3.86 ± 1.17	3.64 ± 1.16 (5.7%)	3.22 ± 1.02*(16%)	**1.93 ± 0.96***(49%)
Mean improvement		3.4%	7.3%	30%
G2 simulated signals (SNRs)	NO DEC + HPF			
-5 dB	19.8 ± 6.36	21.2 ± 7.55 (-7%)	17.5 ± 6.63 (12%)	**16.5 ± 5.16***(16%)
0 dB	12.7 ± 3.99	13.1 ± 4.56 (-3.1%)	12.1 ± 4.83 (4.7%)	**10.8 ± 3.31***(15%)
5 dB	9.08 ± 2.88	9.23 ± 3.08 (-1.6%)	8.64 ± 2.90 (4.8%)	**7.92 ± 3.12** (13%)
10 dB	7.67 ± 2.44	7.54 ± 2.47 (1.7%)	7.27 ± 2.69 (5.2%)	**7.03 ± 2.39** (8.3%)
Mean improvement		-2.5%	6.7%	13%
Real signals (noise elimination)				
ARR	1.94±2.20	2.77±2.98	2.38±2.72	**4.54±6.33***
ARR_{qrs}	8.66±10.2	8.17±6.71	7.60±8.51	**9.37±7.60**

of power of two in the scale factors in DWT, an imposition that yields only four subcomponents between 0.5 and 8 Hz. But as the energy distribution within this range of frequencies is variable, an optimal separation of the EEG bands may require a different number of subcomponents. The adaptive manner of decomposing signals by the EMD and CEEMDAN is, therefore, more convenient to separate and reassemble the subcomponents as a function of f_e, the frequency containing the ECG artifacts. Other wavelet-based methods not explored here, such as the wavelet packet transform, could be employed alternatively to obtain more subcomponents in the aforementioned range. However, finding the optimal basis in this solution is not straightforward.

The major issue of EMD, mode mixing, has not been found to be a major concern in the application presented herewith. The main problem was rather to have IMFs with oscillations crossing the threshold established by f_e, critical mixing, a fact that is not necessarily related to mode mixing. By quantifying critical mixing, we corroborated that the CEEMDAN, thanks to its superior performance, reduces this effect and provides the best denoising results.

However, the use of decomposition techniques introduce some limitations that should be taken into account. Firstly, distortion in low frequency bands cannot be completely avoided since the rejection of subcomponents below 0.5 Hz implies the removal of certain content over this frequency. Although this limitation is partially solved by the enhanced spectral separation of CEEMDAN, the degree of rejected true slow-delta waves needs to be studied in future works because not only technical, but also physiological and maturational considerations appear on the scene [24]. But we also would like to note that in less noisy environments the low frequency limit could be decreased below 0.5 Hz to include the slowest delta content. Secondly, the choice of CEEMDAN implies an increased computational cost, but even if a recent algorithm has reduced its complexity, it is still may be considered a drawback for current real-time systems. In the near future, the application of the family of EMD methods to denoise EEG is more plausible for the NICU as the algorithm continues to be improved in terms of speed and bedside equipment is becoming more powerful.

Conflict of interest

There are no known conflicts of interest associated with this publication and there has been no significant financial support for this work that could have influenced its outcome. The database involved in this study received the ethic approval by the Regional Ethics Committee (Comité de Protection des Personnes, CPP Ouest 6-598).

Acknowledgements

The research for this paper was financially supported by the project INTEM between Rennes University Hospital and the LTSI-INSERM U1099. X. Navarro is currently funded by Air Liquide Medical Systems France through the COVEM Project.

References

[1] D. Maynard, P. F. Prior and D. F. Scott. Device for continuous monitoring of cerebral activity in resuscitated patients. *British Medical Journal*, 4(5682): 545–546, 1969.

[2] C. F. Hagmann, N. J. Robertson and D. Azzopardi. Artifacts on Electroencephalograms May Influence the Amplitude-Integrated EEG Classification: A Qualitative Analysis in Neonatal Encephalopathy. *Pediatrics*, 118(6):2552–4, 2006.

[3] P. Celka, B. Boashash, and P. Colditz. Preprocessing and time-frequency analysis of newborn EEG seizures. *IEEE Engineering in Medicine and Biology Magazine*, 20(5):30–39, 2001.

[4] N. Erdol and F. Basbug. Wavelet transform based adaptive filters: analysis and new results. *IEEE Transactions on Signal Processing*, 44(9):2163–2171, 1996.

[5] S. Hosur and A.H. Tewfik. Wavelet transform domain adaptive FIR filtering. *IEEE Transactions on Signal Processing*, 45(3):617–630, 1997.

[6] T. P. Jung, S. Makeig, C. Humphries, T. W. Lee, M. J. McKeown, V. Iragui, and T. J. Sejnowski. Removing electroencephalographic artifacts by blind source separation. *Psychophysiology*, 37(2):163–178, 2000.

[7] F. Porée, A. Kachenoura, H. Gauvrit, C. Morvan, G. Carrault, and L. Senhadji. Blind source separation for ambulatory sleep recording. *IEEE Transactions on Information Technology in Biomedicine*, 10(2):293–301, 2006.

[8] N. E. Huang, Z. Shen, S. R. Long, M. C. Wu, H. H. Shih, Q. Zheng, N-C. Yen, C. C. Tung, and H. H. Liu. The empirical mode decomposition and the hilbert spectrum for nonlinear and non-stationary time series analysis. *Proceedings of the Royal Society of London. Series A: Mathematical, Physical and Engineering Sciences*, 454(1971):903–995, 1998.

[9] Z. Wu and N. E. Huang. Ensemble Empirical Mode Decomposition: A noise-assisted data analysis method. *Advances in Adaptive Data Analysis*, 01(01):1, 2009.

[10] M. E. Torres, M. A. Colominas, G. Schlotthauer, and P. Flandrin. A complete ensemble empirical mode decomposition with adaptive noise. In *2011 IEEE International Conference on Acoustics, Speech and Signal Processing (ICASSP)*, pages 4144–4147. IEEE, 2011.

[11] S. Pal and M. Mitra. Empirical mode decomposition based ECG enhancement and QRS detection. *Computers in Biology and Medicine*, 42(1):83–92, 2012.

[12] J. P. Lindsen and J. Bhattacharya. Correction of blink artifacts using independent component analysis and empirical mode decomposition. *Psychophysiology*, 47(5):955–960, 2010.

[13] B. Mijović, M. De Vos, I. Gligorijević, J. Taelman and S. Van Huffel. Source Separation From Single-Channel Recordings by Combining Empirical-Mode Decomposition and Independent Component Analysis *IEEE Transactions on Biomedical Engineering*, 57(9):2188–2196, 2010.

[14] X. Navarro, F. Porée, and G. Carrault. ECG removal in preterm EEG combining empirical mode decomposition and adaptive filtering. In *2012 IEEE International Conference on Acoustics, Speech and Signal Processing (ICASSP)*, pages 661–664, 2012.

[15] J. M. Stern. Atlas of EEG Patterns. *Lippincott Williams & Wilkins*, 2005.

[16] S. Mallat. A wavelet tour of signal processing *Academic press*, 1999.

[17] I. Daubechies. *Ten Lectures on Wavelets*. SIAM: Society for Industrial and Applied Mathematics, 1 edition, 1992.

[18] J.P Turnbull, K.A Loparo, M.W Johnson, and M.S Scher. Automated detection of tracé alternant during sleep in healthy full-term neonates using discrete wavelet transform. *Clinical Neurophysiology*, 112(10):1893–1900, 2001.

[19] G. Rilling, P. Flandrin, and P. Gonçalvès. On empirical mode decomposition and its algorithms. In *Proceedings of the 6th IEEE/EURASIP Workshop on Nonlinear Signal and Image Processing (NSIP '03), Grado, Italy*, 2003.

[20] M. A. Colominas, G. Schlotthauer and M. E. Torres Improved complete ensemble EMD: A suitable tool for biomedical signal processing *Biomedical Signal Processing and Control*, 14: 19–29, 2014

[21] S. Haykin. *Adaptive Filter Theory*. Pearson Education, 4 edition, 2002.

[22] E. Eleftheriou and D.D. Falconer. Tracking properties and steady-state performance of RLS adaptive filter algorithms. *IEEE Transactions on Acoustics, Speech and Signal Processing*, 34(5):1097–1110, 1986.

[23] S. Puthusserypady and T. Ratnarajah. Robust adaptive techniques for minimization of EOG artefacts from EEG signals. *Signal Processing*, 86(9):2351–2363, 2006.

[24] M.D Lamblin, M. André, M.J Challamel, L. Curzi-Dascalova, A.M. d'Allest, E. De Giovanni, F. Moussalli-Salefranque, Y. Navelet, P. Plouin, M.F Radvanyi-Bouvet, D. Samson-Dollfus and M.F. Vecchierini-Blineau. Electroencephalography of the premature and term newborn. Maturational aspects and glossary. *Neurophysiol Clin.*, 29(2):123–219, 1999.